J. Biochem. 2009;146(1)77–85
doi:10.1093/jb/mvp048

Influence of Magnesium Ion on the Binding of p53 DNA-Binding Domain to DNA-Response Elements

Yonglai Xue, Shuai Wang and Xizeng Feng*
College of Life Science, Nankai University, Tianjin, 300071, P. R. China

Received January 14, 2009; accepted March 2, 2009; published online March 18, 2009

Site-specific recognition and DNA-binding activity of p53 are crucial for its tumour suppressor function. Previous reports have shown that metal ions can affect the specific recognition and DNA-binding activity of p53DBD. Here we firstly report that magnesium ion can bind to the protein and influence its DNA-binding activity. To elucidate the nature and the effect of metal ions in the reaction chemistry, we utilized endogenous tryptophan fluorescence to quantitate the interaction between p53DBD and metal ions. The K_a value for the binding of Mg^{2+} to the protein is $1.88 \times 10^3\,M^{-1}$. Analysis of the CD data clearly suggested that the binding of magnesium ion induced a subtle conformational change rather than a radical modification of the overall protein architecture. Based on the results of electrophoretic mobility shift assays and fluorescence experiments, we concluded that the binding of Mg^{2+} significantly stimulated the binding of the protein to DNA in a sequence-independent manner, which differed from that of zinc ions in a sequence-specific manner. Based on these results and the fact that Mg^{2+} exists at relatively high concentration in the cell, we propose that Mg^{2+} is one of potential factors to affect or regulate the transactivation of p53.

Key words: affinity, association constant, conformational change, DNA-binding activity, fluorescence, protein–DNA interaction.

Abbreviations: CD, circular dichroism; DBD, DNA-binding domain; DTT, dithiothreitol; EDTA, ethylenediaminetetraacetic acid; RGC, ribosomal gene cluster; SDS, sodium dodecyl sulfate; UV, ultraviolet.

The tumour suppressor protein p53 is a widely distributed phosphoprotein which functions to maintain the integrity of the genome (*1–4*). It acts as a sequence-specific transcription factor which is activated in response to a variety of DNA damaging agents, and may lead to cell cycle arrest at the G1/S phase checkpoint, DNA repair or induction of apoptosis (*5–10*). Virtually all of these presently known biological functions of p53 depend critically upon its DNA-binding properties (*11–13*). Wild-type p53 consists of three major functional domains, the C-terminal tetramerization domain, the N-terminal transactivation domain and the central DNA-binding domain (p53DBD) encompassing amino-acid residues from 96 to 308 (*4*, *14*). p53 is mutated in more than half of the human cancers (*15*). The overwhelming majority of these mutations occurs in the sequence-specific DNA-binding domain and result in the complete or partial loss of its DNA-binding activity (*4*, *16*). Therefore, site-specific recognition and DNA-binding activity of p53 are crucial for its tumour suppressor function (*5*, *17*).

Wild-type p53 binds as a tetramer (*18–21*) to over 100 naturally occurring response elements associated with different specific functions, and human genome contains ~200–300 such sites (*22*). Most of the p53-response elements identified in human genome are 20-bp sequences, containing two decameric half sites, following the consensus pattern RRRC(A/T)|(T/A)GYYY, where R and Y denote purine and pyrimidine base respectively, and the vertical bar indicates the center of pseudodyad symmetry (*18*). These decamers may be separated by up to 21 bp without complete loss of p53-binding affinity (*23*), but the functional sites have shorter intervening spacers and only one copy of these decameric half-sites is insufficient for the functional binding of p53 (*22*). C(A/T)|(T/A)G in the consensus pattern RRRC(A/T)|(T/A)GYYY can exhibit a large flexibility for bending or kinking into the major groove (*24–26*). The fact that many architectural proteins utilize CA|TG dimers (*27–29*), suggests that these dimers may play an important role in specific DNA recognition by transcription factors, especially the functional multiplicity of p53.

Proper conformation of the p53 DNA-binding domain is necessary for DNA binding and transactivation of target genes. The crystal structure of p53DBD reveals that the p53 core domain structure consists of a beta sandwich that serves as a scaffold for two large loops (L2 and L3) and a loop–sheet–helix motif (L1) (Fig. 1) (*30*). The loop–sheet–helix motif contacts the DNA major groove, while L3 loop binds the DNA minor groove. Zn^{2+} is coordinated to C176 and H179 of the L2 loop and to C238 and C242 of the L3 loop. Thus, zinc appears to hold the L3 loop in the proper orientation for the minor groove binding. Zinc coordination is thought to be necessary for transcriptional activation and removal of zinc reduces the DNA-binding specificity (*31–36*). Nevertheless, the binding of mercury, cadmium (*33*, *34*) and copper (*37–38*) to the

*To whom correspondence should be addressed. Tel: +86-22-2350-7022, Fax: +86-22-2350-7022,
E-mail: xzfeng@nankai.edu.cn

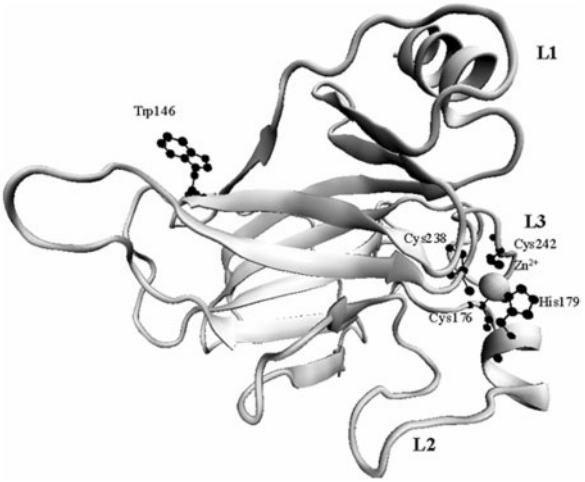

Fig. 1. **A, X-ray crystal structure of p53DBD (*30*). Residues coordinated zinc ion are labelled and shown as stick models.** Trp-146 is also shown, which was used as a fluorescent probe.

protein results in disrupting the p53 conformation and the DNA-binding activity. The opposite effects of metal ions on p53 support the notion that additional metal ions or cellular factors can affect specific recognition.

In this study, we discovered that magnesium ion could bind to the p53DBD protein and affect the affinity of p53DBD binding to the DNA-response elements. To elucidate the nature and the role of magnesium ion in the reaction chemistry, we have utilized endogenous tryptophan fluorescence to evaluate the interactions between metal ions and p53DBD and the influence of metal ions on the DNA-binding affinity of p53DBD. Based on the results of electrophoretic mobility shift assays and fluorescence experiments, we concluded that the binding of Mg^{2+} enhanced the binding of the protein to DNA in a sequence-independent manner, which differed from that of zinc ions in a sequence-specific manner.

MATERIALS AND METHODS

Expression and Purification of p53DBD—The p53DBD cDNA-encoding amino-acid residues 96–308 was cloned in the pET32a expression vector (Novagen). The recombinant plasmids were transformed into *Escherichia coli* BL21 (DE3) trx B^-. The cells were incubated in LB medium at 37°C and induced by 0.25 mM isopropyl β-D-thiogalactoside (IPTG) and then cultured at 25°C for 7 h. The cells were harvested by centrifugation and lysed by osmotic shock method. The recombinant proteins were purified by two chromatographic steps: affinity chromatography and gel filtration chromatography. The pooled fractions from the gel filtration column were digested with enterokinase at 25°C for 7 h. The digested protein was further purified further on a Sephadex G-75 gel filtration column in buffer G (50 mM Tris–HCl, pH 7.5, 100 mM NaCl, 1 mM DTT). The final purified p53DBD was checked on an SDS–polyacrylamide gel for purity. To remove Zn^{2+}, the p53DBD protein was treated with 2.5 mM EDTA, and then passed through a column of Sephadex G-75 equilibrating in buffer G. The protein concentration was determined by the Bradford method with bovine serum albumin as the standard.

Fluorescence Measurements—All the fluorescence measurements were performed on a Hitachi F-4500 fluorescence spectrophotometer using an excitation wavelength of 295 nm at room temperature. Emission spectra were recorded from 310 nm to 450 nm. The excitation and the emission bandwidths were both set on 5 nm. Each data point reported was an average of three determinations. All the protein concentrations were 1.8 μM in buffer G (50 mM Tris–HCl, pH 7.5, 100 mM NaCl, 1 mM DTT). Either the buffer solution alone or the buffer containing the appropriate quantity of substrate was subtracted from the fluorescence spectra to obtain the final results.

Fluorescence quenching is a decrease of the quantum yield of the fluorescence caused by a variety of molecular interactions, including excited-state reactions, molecular rearrangements, energy transfer, ground-state complex formation and collisional quenching. The different mechanisms of quenching are usually classified as dynamic quenching and static quenching. Dynamic quenching refers to a process that the fluorophore and the quencher contact during the transient existence of the excited state. Both static and dynamic processes are described by the well-known Stern–Volmer equation as Eq. 1.

$$\frac{F_0}{F} = 1 + K_q \tau_0 [Q] = 1 + K_{SV}[Q] \quad (1)$$

where, F_0 and F are the fluorescence intensities of p53DBD in the absence and presence of the quencher, respectively. K_q is the quenching rate constant of the biomolecule, K_{SV} is the Stern–Volmer quenching constant, τ_0 is the average lifetime of the biomolecule without the quencher, and $[Q]$ is the concentration of the quencher.

Static quenching refers to fluorophore–quencher complex formation. In a static quenching process, on the assumption that there are n substantive ligand-binding sites on the p53DBD protein, the quenching reaction can be shown as Eq. 2.

$$nQ + \text{p53DBD} \rightleftharpoons Q_n \cdot \text{p53DBD} \quad (2)$$

The binding constant K_a can be calculated as Eq. 3.

$$K_a = \frac{[Q_n \cdot \text{p53DBD}]}{[Q]^n [\text{p53DBD}]} \quad (3)$$

where K_a is the association constant, [p53DBD] and $[Q]$ are the concentration of the free protein and ligand, respectively, $[Q_n \cdot \text{p53DBD}]$ is the concentration of protein complex. Given that the total protein concentration is equal to the sum of the free protein and protein complex concentration, the Eq. 3 can be changed to Eq. 4.

$$K_a = \frac{[\text{p53DBD}]_{tot} - [\text{p53DBD}]}{[Q]^n \cdot [\text{p53DBD}]} \quad (4)$$

The fluorescence intensity is proportional to the concentration of protein, which is describes as Eq. 5.

$$\frac{[\text{p53DBD}]}{[\text{p53DBD}]_{tot}} = \frac{F}{F_0} \quad (5)$$

Equations 4 and 5 can then be combined to give Eq. 6.

$$\mathrm{Log}\,\frac{F_0 - F}{F} = \mathrm{Log}\,K_a + n\,\mathrm{Log}\,[Q] \qquad (6)$$

where n is the number of binding sites. K_a and n will be derived from the intercept and slope of a linear plot of $\log(F_0 - F)/F$ versus log[ligand] based on Eq. 6.

Analysis of Competitive Binding—The analysis of the effect of two metal ions, Zn^{2+} and Mg^{2+} was performed in a method analogous to the previous report to analyse the kinetics of a system in which two alternative substrates compete for the same enzyme-binding site (*39–40*). Typical experimental procedure is that: Add an aliquot of Mg^{2+} to 1.8 μM p53DBD in the standard buffer G. Measure the fluorescence changes produced. Then proceed with a standard single ligand titration with Zn^{2+}. The concentrations of Mg^{2+} used in each set of experiments were 0 μM, 25 μM, 50 μM and 100 μM.

Circular Dichroism Spectroscopy Measurements—Circular dichroism measurements were performed on a Jasco J-715 spectropolarimeter. Typical scans were measured at the rate of 200 nm/min with cell path lengths of 1 and 10 mm for far- and near-UV CD measurements, respectively. Each CD spectrum given was an average of six scans at room temperature. The final protein concentration was 8 μM and 22 μM in buffer G (50 mM Tris–HCl, pH 7.5, 100 mM NaCl, 1 mM DTT) with or without 100 μM metal ions for far- and near-UV CD measurements, respectively. All of the dichroic spectra were corrected by subtracting the background spectrum. The ellipticity results were expressed as mean residue ellipticity, $[\theta]$, in degrees $cm^2\ dmol^{-1}$.

Electrophoretic Mobility Shift Assays—The pEGFP-C2 plasmid was prepared by an alkaline lysis procedure. The purified plasmids (30 nM) were incubated with 1.8 μM p53DBD in buffer G under the condition of different concentrations of metal ions for 30 min at room temperature. Then the samples were determinated by electrophoretic mobility shift assays.

Zeta Potential Measurements—The zeta potential of the p53DBD protein was performed by ZetaPlus zeta potential analyzer at 10°C. The protein alone or incubated with 100 μM metal ions on the ice for 30 min were used. Zeta potential values were calculated from measured velocities using the Smoluchowski equation, and the results are expressed as a mean of three runs.

RESULTS AND DISCUSSION

Expression, Purification and Intrinsic Fluorescence Properties of Tumour Suppressor Protein p53DBD—The p53DBD protein contains a beta sandwich that supports two large loops and a loop–sheet–helix motif, and its activity depends on the presence of zinc ion (*33–36*). To explore whether additional cellular factors existed influence the affinity of p53DBD protein binding to the DNA-response elements, a truncated form of p53DBD encoding amino-acid residues 96–308 was expressed and purified (*41–43*). SDS–PAGE analysis showed that the 24-kDa p53DBD protein was the predominant polypeptide in the purified fraction (Fig. 2A). The concentration of p53DBD protein in this fraction was estimated to be 170 μg/ml.

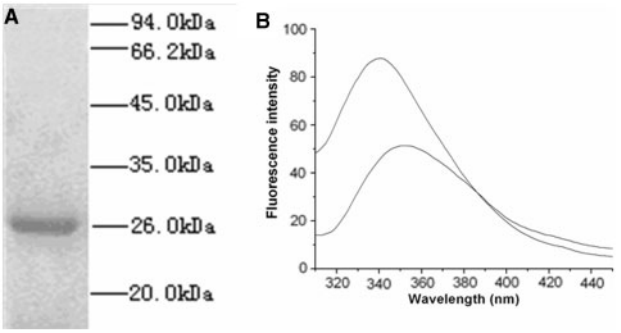

Fig. 2. **Expression, purification and intrinsic fluorescence properties of p53DBD.** (A) the purified p53DBD was analysed by electrophoresis through a 12.5% polyacrylamide gel containing 0.1% SDS and visualized with Coomassie Blue Dye. The positions and sizes (in kDa) of the size markers are indicated on the right. (B) background corrected fluorescence emission spectrum of the purified p53DBD. The upper curve: 1.8 μM p53DBD in 50 mM Tris–HCl, pH 7.5, 100 mM NaCl, 1 mM dithiothreitol at room temperature. The lower curve: 1.8 μM p53DBD was treated with 4.2 M GdmHCl for 1 h at room temperature. Fluorescence spectrum was recorded at an excitation wavelength of 295 nm.

The fluorescence emission spectrum of the purified p53DBD in standard buffer G at room temperature is shown in Fig. 2B. The excitation was carried out at 295 nm, where there are no other residues being excited but tryptophan. According to previous report (*44*), the emission spectral maximum wavelength is at 330–332 nm, which represents that the tryptophan residue is buried in the non-polar regions of the protein. When the emission spectral maximum wavelength is located in 340–342 nm, it suggests that the tryptophan residue is in limited contact with water which is probably immobilized by bonding at the protein surface. When the maximum wavelength is located in 350–353 nm, it means that the tryptophan residue is completely exposed to water. Analysis of the fluorescence emission spectra of p53DBD showed that the recombinant protein exhibited a maximum at 340 nm when excited at 295 nm. This is in agreement with the p53DBD crystal structure in which the tryptophan residue is located in the surface of the protein (Fig. 1) (*30*). After denaturing with 4.2 M GdmHCl for 1 h, there was a distinct red-shifting of the maximum emission fluorescence to 352 nm and the fluorescence intensity decreased at the same time, reflecting the transfer of tryptophan residues to a more polar environment.

Binding of Magnesium Ion to the Tumour Suppressor Protein p53DBD—Previous reports have shown that the bindings of metal ions to proteins could result in a significant decrease in fluorescence emission intensities (*40*, *45–46*). We observed that the fluorescence intensities of p53DBD decreased with increasing concentrations of both Zn^{2+} and Mg^{2+}. Figure 3A and B show the fluorescence decay curves of p53DBD titrated with increasing amounts of Zn^{2+} and Mg^{2+}, respectively. The addition of increasing amounts of metal ions produced a decrease in the fluorescence intensities, but the emission maximum (340 nm) and spectral bandwidth

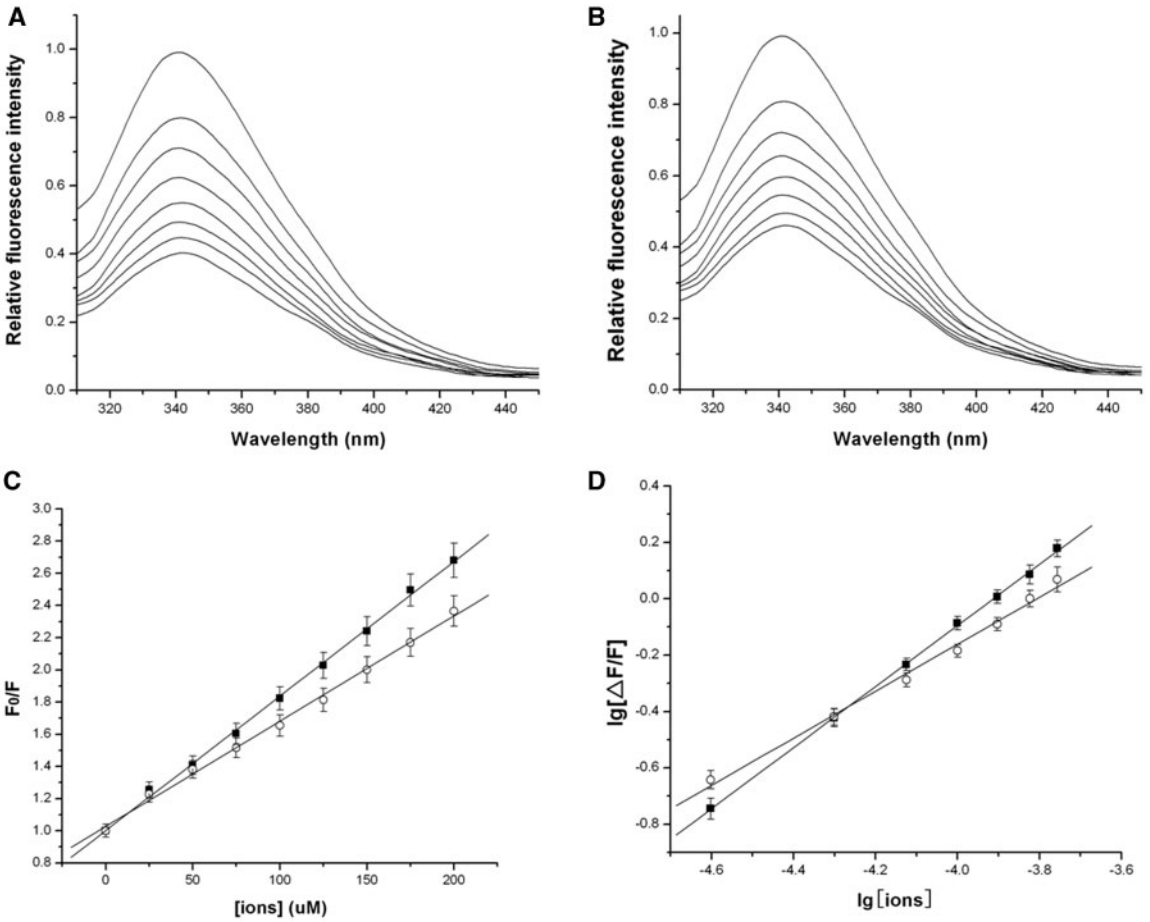

Fig. 3. **Titration of p53DBD with Mg^{2+} ions.** (A) increasing amounts of Zn^{2+} were added to a 1.8 μM solution of the protein in binding buffer G. (B) increasing amounts of Mg^{2+} were added to a 1.8 μM solution of the protein in binding buffer G. (C) Stern–Volmer plots of fluorescence quenching of p53DBD with Zn^{2+} (filled square) and Mg^{2+} (open circle). (D) Logarithmic plots of fluorescence quenching of p53DBD treated with Zn^{2+} (filled square) and Mg^{2+} (open circle).

were not affected. Fluorescence spectroscopy is very sensitive to the changes in the environment of aromatic amino-acid residues. Thus, Trp fluorescence can be used as a probe to monitor the change in the tertiary structure of p53DBD caused by metals binding (*47*). The fact that increasing amounts of metal ions produced a decrease in the fluorescence intensities suggested that the binding of metal ions to p53DBD changed the microenvironment of tryptophan residue and the tertiary structure of the protein.

The Stern–Volmer quenching constants K_{SV} were determined by Eq. 1 (Fig. 3C). According to the literature (*48*), the τ_0 of biomolecule is about 10^{-8} s, so the quenching rate constants K_q can be calculated and summarized in Table 1. Generally, the maximum scatter collision quenching constant, K_q, of various kinds of quenchers with biomolecule is 2.0×10^{10} l $mol^{-1} s^{-1}$ (*49*). As can be seen in Table 1, the rate constants for the quenching of the protein caused by the two metal ions are greater than the K_q for the scatter mechanism. These data suggest that the fluorescence quenching is not the result of dynamic collision quenching, but static quenching.

Table 1. **Association constants (K_a), dissociation constants (K_d), the number of binding site n and quenching rate constant K_q of metal ions to p53DBD.**

Ion	K_a (M^{-1})	K_d (M)	n	K_q (l $mol^{-1} s^{-1}$)
Zn^{2+}	1.74×10^4	5.75×10^{-5}	1.07	8.37×10^{11}
Mg^{2+}	1.88×10^3	5.32×10^{-4}	0.86	6.55×10^{11}

In the static quenching process, the number of binding site n and the association constant K_a could be calculated according to Eq. 6. The logarithmic plots of $\log(F_0 - F)/F$ versus log[ions] are shown in Fig. 3D and the related data are summarized in Table 1. As can be seen in Table 1, the association constant of the protein with Mg^{2+} and Zn^{2+} are $1.88 \times 10^3 M^{-1}$ and $1.74 \times 10^4 M^{-1}$, respectively. The binding affinity of Zn^{2+} to p53DBD is 9-fold greater than that of Mg^{2+}.

Analysis of Competitive Binding—Previous studies showed that mercury and cadmium could substitute for zinc but disrupt the p53 conformation and specific DNA-binding activity (*33–34*). Our results showed that Mg^{2+} could bind to p53DBD. We were thus interested in

determining whether the two metal ions bind to the same active site on the protein or not. Competitive alternative ligand-binding experiments (*39–40*) were carried out to determine whether the two metal ions compete for a common binding site. In the initial experiment, the addition of increasing amounts of Zn^{2+} to the protein in the absence of Mg^{2+} resulted in the changes in fluorescence (ΔF) produced at 340 nm. Then the titrations were carried out in the presence of three concentrations of Mg^{2+}. The change in fluorescence (ΔF) was plotted against the concentration of zinc ions. The saturation isotherm resulting from the competitive ligand experiment was shown in Fig. 4. The pattern of lines is in accordance with a model in which the binding of Zn^{2+} and Mg^{2+} is mutually exclusive (*39*). It suggests that magnesium competes with zinc for binding to p53DBD.

Circular Dichroism Analysis of Magnesium Ions Binding to p53DBD—Intrinsic fluorescence change shows the local environment change of the tryptophan residue, which provides a measure of the tertiary conformation of p53DBD. To further characterize the interaction between the magnesium ions and p53DBD, far- and near-UV CD spectra were adopted. Analysis of the far-UV CD spectra (Fig. 5A) revealed that the binding of Mg^{2+} to p53DBD induced a slightly decrease of the ellipticity in the region of 200–230 nm like Zn^{2+}. This suggested that the binding of both the two metal ions led to a minor decrease in α-helical structure of the protein molecule. As can be seen in Fig. 5B, similar to the binding of Zn^{2+} to p53DBD, the binding of Mg^{2+} resulted in a reduction of the amplitude of the signal. The similar results were seen in other ion-binding proteins (*40*). The results of near-UV CD confirm that the decrease of fluorescence intensity observed upon the binding of metal ions is indeed reflecting conformational changes. Taken together, the data from both CD spectra and fluorescence studies indicate that the binding of the two metal ions induce a subtle conformational change rather than a radical modification of the overall protein architecture.

Influence of Magnesium Ion on the DNA-Binding Activity of p53DBD—Zinc coordination has been shown to be necessary for the specific DNA binding, while the binding of mercury, cadmium and copper to the protein results in disrupting DNA-binding activity (*31–38*). We were thus interested in determining whether the binding of Mg^{2+} to the protein could affect the affinity of p53DBD binding to the DNA sites, an essential step in the initiation of transcription. Fluorescence spectroscopy and electrophoretic mobility shift assays were performed to determine the effect of magnesium ions.

Two consensus DNA-response elements: the p21/waf1/cip1-response element (5′-GAACATGTCCCAACATGT

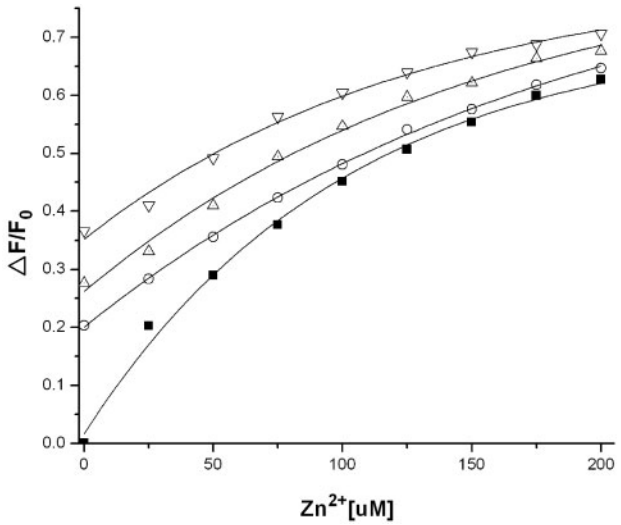

Fig. 4. **Dual ligand titration using Zn^{2+} and Mg^{2+}.** Standard titration assays were to add Zn^{2+} ions to p53DBD in the presence of increasing amounts of Mg^{2+} ions. The concentrations of Mg^{2+} used in these experiments were 0 μM (filled square), 25 μM (open circle), 50 μM (open triangle) and 100 μM (open inverted triangle).

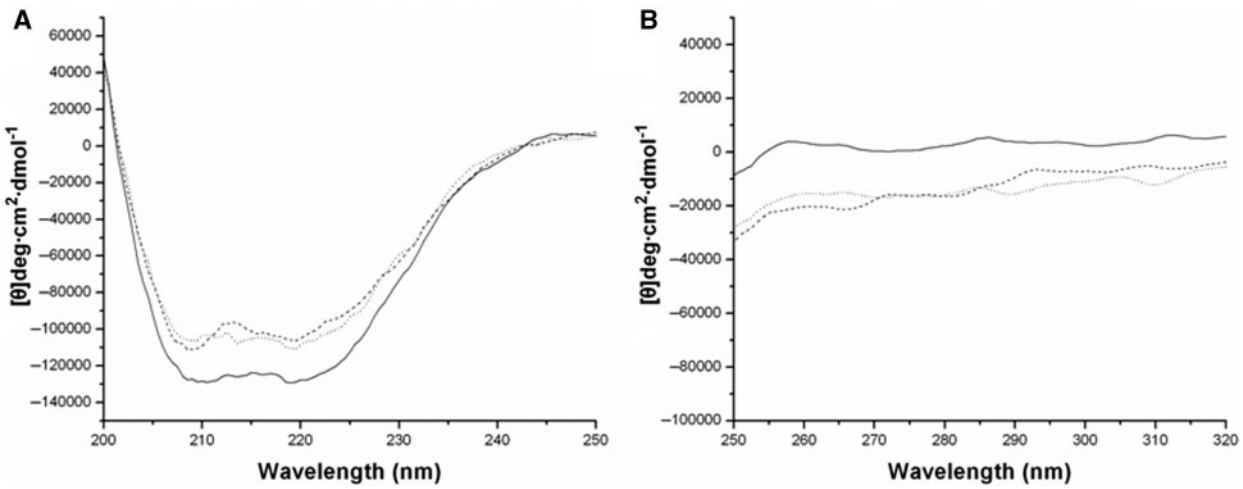

Fig. 5. **Effect of metal ions binding on far- (A) and near-UV (B) circular dichroism spectra of p53DBD at room temperature in buffer G.** Spectra were collected under different metal content: no ions added (solid lines), 100 μM Zn^{2+} added (dashed lines) and 100 μM Mg^{2+} added (dotted lines).

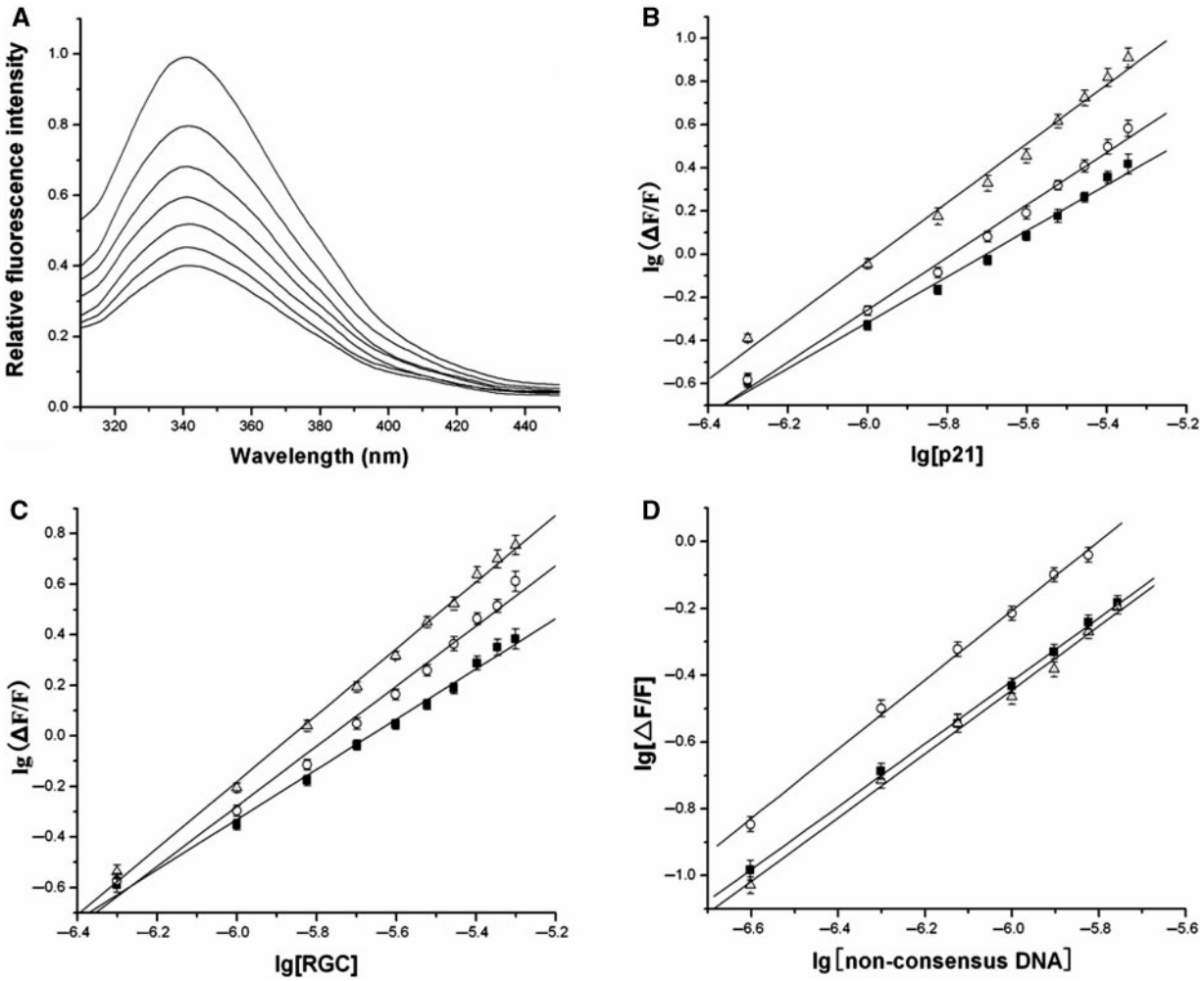

Fig. 6. **Titration of p53DBD with DNA-response elements.** (A) increasing amounts of *p21/waf1/cip1* were added to a 1.8 μM solution of the protein. (B, C and D) Logarithmic plots of fluorescence quenching of p53DBD titrated with different DNA-response elements in the absence (filled circle) and presence of Zn^{2+} (open triangle) or Mg^{2+} (open circle).

TG-3′) and the ribosomal gene cluster (RGC) sequence (5′ -TGCCTTGCCTGGACTTGCCT-3′) and a non-consensus DNA sequence (5′ -GGTTTGAATAAAGAGTAA AGAT-3′) were used in fluorescence spectroscopy assays (*50–51*). Initial experiment performed in the absence of metal ions, the p21/waf1/cip1-response element, as a ligand, was added to a fixed concentration of p53DBD which resulted in a significant decrease in emission fluorescence intensities gradually (Fig. 6A). The fluorescence quenching data were analysed by the Stern–Volmer equation and K_q was summarized in Table 2. The quenching rate constant of the protein caused by p21/waf1/cip1 was also greater than the K_q for the scatter mechanism. It suggested that the fluorescence quenching was caused by static quenching. The logarithmic Eq. 6 thus can be used to determine the association constant K_a. To determine the role of metal ions, we performed the titration experiment again in the presence of 100 μM $ZnCl_2$ or $MgCl_2$ (details in Supplementary Data). The titration experiments of RGC and non-consensus DNA sequence were performed by similar methods. The logarithmic plots of $\log(F_0 - F)/F$ versus lg[DNA] were shown in Fig. 6 and the related data were summarized in Table 2.

The p53DBD protein associates with p21/waf1/cip1 and RGC in the absence of metal ions with mean equilibrium dissociation constants of 8.93×10^{-7} M and 2.39×10^{-6} M, respectively. The equilibrium dissociation constants determined for the p21/waf1/cip1-response element and RGC in the presence of Zn^{2+} are altered to 7.04×10^{-9} M and 1.86×10^{-8} M, which are in general agreement with the results reported before from quantitative gel mobility retardation assay of K_d 7.8×10^{-9} M and 1.8×10^{-8} M for p21/waf1/cip1 and RGC (*42*). However, the p53DBD possess similar K_d values for the non-consensus DNA sequence in the absence and the presence of Zn^{2+}. Our experiments also prove that zinc is crucial for the sequence-specific DNA-binding affinity of p53DBD.

Surprisingly, the equilibrium dissociation constants of p53DBD with p21/waf1/cip1 and RGC are altered to 9.17×10^{-8} M and 1.41×10^{-7} M as a result of adding Mg^{2+}. The p21/waf1/cip1-response element has a 10-fold higher affinity in the existence of Mg^{2+}, while RGC has a 16-fold higher affinity. Moreover, the equilibrium

Table 2. **Association constants (K_a), dissociation constants (K_d), quenching rate constant (K_q) and the free energy of the binding of p53DBD to different DNA-response elements in the absence and the presence of metal ions.**

Ligand	K_a (M^{-1})	K_d (M)	ΔG^0 (kJ mol^{-1})	K_q (l mol^{-1} s^{-1})
p21/waf1/cip1	1.12×10^6	8.93×10^{-7}	−34.5	4.91×10^{13}
p21/waf1/cip1 (Zn^{2+})	1.42×10^8	7.04×10^{-9}	−46.5	1.15×10^{14}
p21/waf1/cip1 (Mg^{2+})	1.09×10^7	9.17×10^{-8}	−40.1	6.77×10^{13}
RGC	4.17×10^5	2.39×10^{-6}	−32.1	4.40×10^{13}
RGC (Zn^{2+})	5.37×10^7	1.86×10^{-8}	−44.1	8.61×10^{13}
RGC (Mg^{2+})	7.08×10^6	1.41×10^{-7}	−39.1	6.04×10^{13}
Non-consensus DNA	1.68×10^5	5.95×10^{-6}	−29.8	3.72×10^{13}
Non-consensus DNA (Zn^{2+})	1.93×10^5	5.18×10^{-6}	−30.2	3.52×10^{13}
Non-consensus DNA (Mg^{2+})	1.26×10^6	7.94×10^{-7}	−34.8	6.19×10^{13}

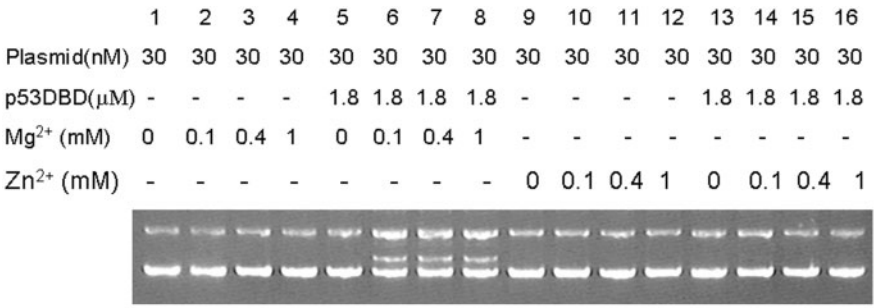

Fig. 7. **Electrophoretic mobility shift assays.** The samples were run on a 1% agarose gel, and the amounts of agents used in the assays are indicated at the top of the gel. The upper band is the open circular DNA and the lower is supercoiled DNA in lane 1.

dissociation constants of p53DBD with non-consensus DNA sequence is also altered from 5.95×10^{-6} M to 7.94×10^{-7} M in the presence of Mg^{2+}. These results clearly indicate that the binding of magnesium ion can enhance the DNA-binding affinity of p53DBD in a sequence-independent manner.

To further confirm that the influence of magnesium ions on the DNA-binding affinity of p53DBD is in a sequence-independent manner, electrophoretic mobility assays were used. The pEGFP-C2 plasmid (4.7 kb) can be used as a long non-consensus DNA. As we can see in Fig. 7, the plasmids were only incubated with Mg^{2+} (lanes 1–4) or Zn^{2+} (lanes 9–12), the bands of plasmids were not affected. When the plasmids were incubated with p53DBD (lanes 5 and 13) in the absence of metal ions, the bands were also unaffected. It is due to that the interaction between the protein and DNA is weak in the absence of metal ions. When the plasmids were incubated with p53DBD in the presence of Zn^{2+} in lanes 14–16, where found no gel retardation. But when the binding reaction was carried out in the presence of Mg^{2+} in lanes 6–8, gel retardation appeared. These results clearly suggest that the binding of magnesium ions enhance the DNA-binding affinity of p53DBD in a sequence-independent manner, which differs from that of zinc ions in a sequence-specific manner.

Possible Mechanism for the Effect of Metal Ions—Zinc ions are frequently found in many proteins, in which they play both the catalytic and structural roles (*52*, *53*). The coordination polyhedron of catalytic zinc is usually dominated by histidine side chains, while the coordination polyhedron of structural zinc is almost exclusively dominated by cysteine thiolates (*54*).

Table 3. **The zeta potential of p53DBD in the absence and the presence of metal ions.**

Sample	Zeta potential (mV)
p53DBD	−23.18
p53DBD·Zn^{2+}	−16.05
p53DBD·Mg^{2+}	−18.28

Generally, structural zinc displays a tetrahedral coordination, as in the 'zinc finger' identified in many transcription factors (*55*, *56*). In p53DBD, Zn^{2+} is coordinated by cysteines 176, 238 and 242 and His179 (*30*). Zinc coordination keeps the L2 and the DNA-binding-L3 loops together and holds the L3 loop in the proper orientation for the minor groove binding (*36*). On the other hand, the results of molecular dynamics simulations show that zinc coordination contributes a stronger positive electrostatic potential of the DNA-contacting surface (*57*). The attraction between Zn^{2+} and the DNA phosphate backbone facilitates insertion of Arg248 into the minor groove and provides the possibility for sequence-specific interactions with the bases in the minor groove (*57*). As can be seen in Table 3, the negative potential of p53DBD decreased after the binding of zinc ions, which is in accordance with that zinc coordination contributes a stronger positive electrostatic potential of the DNA-contacting surface. Similarly, the negative potential of p53DBD reduced upon the binding of magnesium ions.

Many enzymes require Mg^{2+} for their activity, and there are two general mechanisms for such activation (*58*). One mechanism is through allosteric activation in

which binding to one more form of the enzyme in the reaction course or another site in the enzyme induces a change in its conformation. The CD results showed that Mg^{2+} brought about conformational changes in p53DBD, which suggested that this mechanism seemed to be applied to the Mg^{2+}-mediated binding of p53DBD to its cognate DNA site. The other mechanism is through binding to a ligand, thereby making it a suitable substrate, e.g., ATP-Mg^{2+}, DNA-Mg^{2+}. The interaction between DNA and Mg^{2+} is non-specific. The results of electrophoretic mobility shift assays and fluorescence experiments showed that the binding of magnesium ions enhanced the DNA-binding affinity of p53DBD in a sequence-independent manner, which indicated that the latter mechanism was also found in the Mg^{2+}-mediated activation.

CONCLUSION

It is well studied that zinc ion is necessary for specific DNA binding of p53DBD. Compared with Zn^{2+}, Mg^{2+} could also bind to the p53DBD protein and enhance its DNA-binding activity in a sequence-independent manner. Tumour suppressor p53 is a transcription factor that transactivates a wide range of genes, including those in DNA repair, cell-cycle arrest and apoptosis. The role of selectivity in binding to its promoters is related to the binding affinity of p53DBD to the DNA sites. The intracellular free Mg^{2+} concentration in most mammalian cells is between 0.5 and 1 mM and many enzymes appear to require and be regulated by concentrations of Mg^{2+} that are well within the physiological range observed in cells. The large fluxes of Mg^{2+} can cross the cell plasma membrane in either direction following a variety of stimuli, resulting in major changes in total and free Mg^{2+} content within cells (*59*, *60*). The fact that the changes in cellular Mg^{2+} content can result in a modification of the activity for several cellular enzymes support the notion that Mg^{2+} is one of potential factors to affect or regulate the transactivation of p53.

FUNDING

National Natural Science Foundation of China (Grant No. 90403140).

CONFLICT OF INTEREST

None declared.

REFERENCES

1. Vogelstein, B., Lane, D., and Levine, A.J. (2000) Surfing the p53 network. *Nature* **408**, 307–310
2. Lane, D.P. (1992) p53, guardian of the genome. *Nature* **358**, 15–16
3. Levine, A.J. (1993) The tumor suppressor genes. *Annu. Rev. Biochem.* **62**, 623–651
4. Ko, L.J. and Prives, C. (1996) p53: puzzle and paradigm. *Genes Dev.* **10**, 1054–1072
5. Levine, A.J. (1997) p53, the cellular gatekeeper for growth and division. *Cell* **88**, 323–331
6. Ding, H.F. and Fisher, D.E. (1998) Mechanisms of p53-mediated apoptosis. *Crit. Rev. Oncog.* **9**, 83–98
7. El-Deiry, W.S., Tokino, T., Velculescu, V.E., Levy, D.B., Parsons, R., Trent, J.M., Lin, D., Mercer, W.E., Kinzler, K.W., and Vogelstein, B. (1993) WAF1, a potential mediator of p53 tumor suppression. *Cell* **75**, 817–825
8. Harper, J.W., Adami, G.R., Wei, N., Keyomarsi, K., and Elledge, S.J. (1993) The p21 Cdk-interacting protein Cip1 is a potent inhibitor of G1 cyclin-dependent kinases. *Cell* **75**, 805–816
9. Prives, C. and Hall, P.A. (1999) The p53 pathway. *J. Pathol.* **187**, 112–126
10. Vousden, K.H. and Lu, X. (2002) Live or let die: the cell's response to p53. *Nature Rev. Cancer* **2**, 594–604
11. Prives, C. (1994) How loops, β sheets, and α helices help us to understand p53. *Cell* **78**, 543–546
12. Milner, J. (1994) Forms and functions of p53. *Semin. Cancer Biol.* **5**, 211–219
13. Anderson, M.E. and Tegtmeyer, P. (1995) Giant leap for p53, small step for drug design. *BioEssays* **17**, 3–7
14. Bargonetti, J., Manfredi, J.J., Chen, X., Marshak, D.R., and Prives, C. (1993) A proteolytic fragment from the central region of p53 has marked sequence-specific DNA-binding activity when generated from wild-type but not from oncogenic mutant p53 protein. *Genes Dev.* **7**, 2565–2574
15. Hainaut, P., Soussi, T., Shomer, B., Hollstein, M., Greenblatt, M., Hovig, E., Harris, C.C., and Montesano, R. (1997) Database of p53 gene somatic mutations in human tumors and cell lines: updated compilation and future prospects. *Nucleic Acids Res.* **25**, 151–157
16. Pietenpol, J.A., Tokino, T., Thiagalingam, S., El-Diery, W.S., Kinzler, K.W., and Vogelstein, B. (1994) Sequence-specific transcriptional activation is essential for growth suppression by p53. *Proc. Natl Acad. Sci. USA* **91**, 1998–2002
17. Meek, D.W. (1998) Multisite phosphorylation and the integration of stass signals at p53. *Cell. Signalling* **10**, 159–166
18. El-Deiry, W.S., Kern, S.E., Pietenpol, J.A., Kinzler, K.W., and Vogelstein, B. (1992) Definition of a consensus binding site for p53. *Nat. Genet.* **1**, 45–49
19. Halazonetis, T.D. and Kandil, A.N. (1993) Conformational shifts propagate from the oligomerization domain of p53 to its tetrameric DNA binding domain and restore DNA binding to select p53 mutants. *EMBO J.* **12**, 5057–5064
20. Friedman, P.N., Chen, X.B., Bargonetti, J., and Prives, C. (1993) The p53 Protein is an Unusually Shaped Tetramer that Binds Directly to DNA. *Proc. Natl Acad. Sci. USA* **90**, 3319–3323
21. Stenger, J.E., Tegtmeyer, P., Mayr, G.A., Reed, M., Wang, Y., Wang, P., Hough, P.V., and Mastrangelo, I.A. (1994) p53 oligomerization and DNA looping are linked with transcriptional activation. *EMBO J.* **13**, 6011–6020
22. Tokino, T., Thiagalingam, S., El-Deiry, W.S., Waldman, T., Kinzler, K.W., and Vogelstein, B. (1994) p53 tagged sites from human genomic DNA. *Hum. Mol. Genet.* **3**, 1537–1542
23. Waterman, J.L., Shenk, J.L., and Halazonetis, T.D. (1995) The dihedral symmetry of the p53 tetramerization domain mandates a conformational switch upon DNA binding. *EMBO J.* **14**, 512–519
24. McNamara, P.T., Bolshoy, A., Trifonov, E.N., and Harrington, R.E. (1990) Sequence-dependent kinks induced in curved DNA. *J. Biomol. Struct. Dyn.* **8**, 529–538
25. Zhurkin, V.B., Ulyanov, N.B., Gorin, A.A., and Jernigan, R.L. (1991) Static and statistical bending of DNA evaluated by Monte Carlo simulations. *Proc. Natl Acad. Sci. USA* **88**, 7046–7050
26. Nagaich, A.K., Bhattacharyya, D., Brahmachari, S.K., and Bansal, M. (1994) CA/TG sequence at the 5' end of oligo(A)-tracts strongly modulates DNA curvature. *J. Biol. Chem.* **269**, 7824–7833

27. Werner, M.H., Gronenborn, A.M., and Clore, G.M. (1996) Intercalation, DNA kinking, and the control of transcription. *Science* **271**, 778–784
28. Dickerson, R.E. (1998) DNA bending: the prevalence of kinkiness and the virtues of normality. *Nucleic Acids Res.* **26**, 1906–1926
29. Olson, W.K., Gorin, A.A., Lu, X.J., Hock, L.M., and Zhurkin, V.B. (1998) DNA sequence-dependent deformability deduced from protein-DNA crystal complexes. *Proc. Natl Acad. Sci. USA* **95**, 11163–11168
30. Cho, Y., Gorina, S., Jeffrey, P.D., and Pavletich, N.P. (1994) Crystal structure of a p53 tumor suppressor-DNA complex: understanding tumorigenic mutations. *Science* **265**, 346–355
31. Hainaut, P., Butcher, S., and Milner, J. (1995) Temperature sensitivity for conformation is an intrinsic property of wild-typep53. *Br. J. Cancer* **71**, 227–231
32. Pavletich, N.P., Chambers, K.A., and Pabo, C.O. (1993) The DNA-binding domain of p53 contains the four conserved regions and the major mutation hot spots. *Genes Dev.* **7**, 2556–2564
33. Hainaut, P. and Milner, J. (1993) A structural role for metal ions in the "wild-type" conformation of the tumor suppressor protein p53. *Cancer Res.* **53**, 1739–1742
34. Meplan, C., Richard, M.J., and Hainaut, P. (2000) Metalloregulation of the tumor suppressor protein p53: zinc mediates the renaturation of p53 after exposure to metal chelators in vitro and in intact cells. *Oncogene* **19**, 5227–5236
35. Verhaegh, G.W., Parat, M.O., Richard, M.J., and Hainaut, P. (1998) Modulation of p53 protein conformation and DNA-binding activity by intracellular chelation of zinc. *Mol. Carcinog.* **21**, 205–214
36. James, S.B. and Stewart, N.L. (2003) Structure, function, and aggregation of the zinc-free form of the p53 DNA binding domain. *Biochem.* **42**, 2396–2403
37. Hainaut, P., Rolley, N., Davies, M., and Milner, J. (1995) Modulation by copper of p53 conformation and sequence-specific DNA binding: role for Cu(II)/Cu(I) redox mechanism. *Oncogene* **10**, 27–32
38. Verhaegh, G.W., Richard, M.J., and Hainaut, P. (1997) Regulation of p53 by metal ions and by antioxidants: dithiocarbamate down-regulates p53 DNA-binding activity by increasing the intracellular level of copper. *Mol. Cell. Biol.* **17**, 5699–5706
39. Painter, G.R., Wright, L.L., Hopkins, S., and Furman, P.A. (1991) Initial binding of 2'-deoxynucleoside 5'-triphosphates to human immunodeficiency virus type 1 reverse transcriptase. *J. Biol. Chem.* **15**, 19362–19368
40. Bougie, I., Charpentier, S., and Bisaillon, M. (2003) Characterization of the metal ion binding properties of the hepatitis C virus RNA polymerase. *J. Biol. Chem.* **278**, 3868–3875
41. Balagurumoorthy, P., Sakamoto, H., Lewis, M.S., Zambrano, N., Clore, G.M., Gronenborn, A.M., Appella, E., and Harrington, R.E. (1995) Four p53 DNA-binding domain peptides bind natural p53-response elements and bend the DNA. *Proc. Natl Acad. Sci. USA* **92**, 8591–8595
42. Nagaich, A.K., Appella, E., and Harrington, R.E. (1997) DNA bending is essential for the site-specific recognition of DNA response elements by the DNA binding domain of the tumor suppressor protein p53. *J. Biol. Chem.* **272**, 14842–14849
43. Nagaich, A.K., Zhurkin, V.B., Durell, S.R., Jernigan, R.L., Appella, E., and Harrington, R.E. (1997) p53-induced DNA bending and twisting: p53 tetramer binds on the outer side of a DNA loop and increases DNA twisting. *Proc. Natl Acad. Sci. USA* **96**, 1875–1880
44. Burstein, E.A., Vedenkina, N.S., and Ivkova, M.N. (1973) Fluorescence and the location of tryptophan residues in protein molecules. *Photochem. Photobiol.* **18**, 263–275
45. Van der Wolk, J.P.W., Klose, M., de Wit, J.G., den Blaauwen, T., Freudl, R., and Driessen, A. J. M. (1995) Identification of the magnesium-binding domain of the high-affinity ATP-binding site of the Bacillus subtilis SecA protein. *J. Biol. Chem.* **270**, 18975–18982
46. Zhu, C.X., Roche, C.J., and Tse-Dinh, Y.C. (1997) Effect of Mg(II) binding on the structure and activity of Escherichia coli DNA topoisomerase I. *J. Biol. Chem.* **272**, 16206–16210
47. Liu, X., Yang, J., Ghazi, A.M., and Frey, T.K. (2000) Characterization of the zinc binding activity of the rubella virus nonstructural protease. *J. Virol.* **74**, 5949–5956
48. Lakowicz, J.R. (1999) *Principles of Fluorescence Spectroscopy*, 2nd edn, pp. 237–265, Plenum Press, New York
49. Lakowicz, J.R. and Weber, G. (1973) Quenching of fluorescence by oxygen-probe for structural fluctuations in macromolecules. *Biochemistry* **12**, 4161–4170
50. Namba, H., Hara, T., Tukazaki, T., Migita, K., Ishikawa, N., Ito, K., Nagataki, S., and Yamashita, S. (1995) Radiation-induced G1 arrest is selectively mediated by the p53-WAF1/Cip1 pathway in human thyroid cells. *Cancer Res.* **55**, 2075–2080
51. Bargonetti, J., Reynisdottir, I., Friedman, P.N., and Prives, C. (1992) Wild-type p53 site specific binding to cellular DNA is regulated by SV40 T antigen and mutant p53. *Genes Dev.* **6**, 1886–1898
52. Maret, W. (2004) Zinc and sulfur: A critical biological partnership. *Biochemistry* **43**, 3301–3309
53. Coleman, J.E. (1992) Zinc proteins: enzymes, storage proteins, transcription factors, and replication proteins. *Annu. Rev. Biochem.* **61**, 897–946
54. Christianson, D.W. (1991) Structural biology of zinc. *Adv. Protein Chem.* **42**, 281–355
55. Lee, M.S., Gippert, G.P., Soman, K.V., Case, D.A., and Wright, P.E. (1989) Three-dimensional solution structure of a single zinc finger DNA-binding domain. *Science* **245**, 635–637
56. Berg, J.M. (1988) Proposed structure for the zinc-binding domains for transcription factor IIIA and related proteins. *Proc. Natl Acad. Sci. USA* **85**, 99–102
57. Duan, J.X. and Nilsson, L. (2006) Effect of Zn^{2+} on DNA recognition and stability of the p53 DNA-binding domain. *Biochemistry* **45**, 7483–7492
58. De, A., Ramesh, V., Mahadevan, S., and Nagaraja, V. (1998) Mg^{2+} mediated sequence-specific binding of transcriptional activator protein C of bacteriophage Mu to DNA. *Biochemistry* **37**, 3831–3838
59. Romani, A.M. and Scarpa, A. (2000) Regulation of cellular magnesium. *Front Biosci.* **5**, D720–D734
60. Romani, A.M. (2007) Magnesium homeostasis in mammalian cells. *Front Biosci.* **12**, 308–331